

Dependence of the Effective Masses in YbAl_3 on Magnetic Field and Disorder

T. Ebihara,¹ E. D. Bauer,² A. L. Cornelius,³ J. M. Lawrence,^{4,*} N. Harrison,⁵ J. D. Thompson,² J. L. Sarrao,²
M. F. Hundley,² and S. Uji⁶

¹Shizuoka University, Shizuoka 422-8529, Japan

²Los Alamos National Laboratory, Los Alamos, New Mexico 87545, USA

³University of Nevada, Las Vegas, Nevada 89154, USA

⁴University of California, Irvine, California 92697, USA

⁵National High Magnetic Field Laboratory, Los Alamos, New Mexico 87545, USA

⁶National Institute for Materials Science, Tsukuba 305-0003, Japan

(Received 12 September 2002; published 25 April 2003)

The susceptibility and specific heat—and hence the effective mass—of the intermediate valence compound YbAl_3 show anomalous enhancement below the Fermi liquid temperature $T_{\text{coh}} \sim 40$ K. We show that these anomalies are suppressed by alloying in $\text{Yb}_{1-x}\text{Lu}_x\text{Al}_3$ indicating high sensitivity to lattice coherence. The de Haas–van Alphen effective masses for key branches of the Fermi surface are reduced by magnetic fields $B > 40$ T. We argue that this reduction does not arise from $4f$ polarization but reflects renormalization of the quasiparticle states by the field.

DOI: 10.1103/PhysRevLett.90.166404

PACS numbers: 71.18.+y, 71.27.+a, 75.20.Hr, 75.30.Mb

The temperature dependence of the susceptibility $\chi(T)$, specific heat $C(T)$, and valence of intermediate valence (IV) compounds can be fit semiquantitatively, and sometimes quantitatively, by the predictions of the Anderson impurity model (AIM) [1]. Both $\chi(T)$ and $C(T)/T$ increase from a finite value at $T = 0$ to a broad maximum at $T_{\text{max}} \sim T_K/(4-6)$. Recently we have shown [2] for the IV compound YbAl_3 that anomalies occur below 40 K: both $\chi(T)$ and $C(T)/T$ —and hence the effective mass m^* —are larger than the value extrapolated from high temperature, rising to a second maximum at or near $T = 0$ (Fig. 1). The susceptibility anomaly is suppressed and normal IV behavior reestablished by magnetic fields $B > 40$ T [2] (Fig. 1, inset).

Below 40 K the electrical resistivity exhibits T^2 behavior [2] and the low temperature optical conductivity exhibits [3] both a very narrow Drude resonance and a midinfrared peak associated with optical transitions across a renormalized hybridization gap. The mid-IR peak begins to be suppressed, the Drude peak begins to broaden, and the effective mass for the Drude peak (which is $25-30m_e$ at low temperature) decreases for $T > 40$ K. Hence, the anomalous enhancement of the effective mass occurs on the scale of the coherence temperature T_{coh} , defined as the temperature below which the coherent renormalized Fermi liquid is fully established.

The effective masses determined by de Haas–van Alphen (dHvA) measurements [4] in YbAl_3 are also in the range $15-30m_e$. In this paper we show that the effective masses measured by dHvA for a field along the $\langle 111 \rangle$ direction reduce by approximately a factor of 2 in magnetic fields $B > B^* = 40$ T. A field of this magnitude is substantially smaller than the Kondo field $B_K \sim k_B T_K / \mu_B$ for this compound ($T_K = 670$ K [2]) and hence the transition cannot arise from $4f$ polarization. The

field energy $\mu_B B^*$ does, however, correspond to $k_B T_{\text{coh}}$ suggesting that magnetic fields of this magnitude renormalize the quasiparticle states. We also show that the specific heat and susceptibility anomalies are suppressed by alloying for concentrations as small as $x = 0.05$ in $\text{Yb}_{1-x}\text{Lu}_x\text{Al}_3$. This suggests that the anomalous effective mass enhancement observed below T_{coh} is a true coherence effect and very sensitive to lattice order.

Single crystals of YbAl_3 and $\text{Yb}_{1-x}\text{Lu}_x\text{Al}_3$ were grown by the self-flux method, with excess aluminum [4]. The susceptibility was measured using a SQUID magnetometer and the specific heat was measured using a relaxation technique. For dHvA measurements, the crystals were aligned using x-ray diffraction and reduced to the appropriate dimensions using a spark cutter followed by etching in acid solutions. The low-field (13–17 T) and intermediate field (17–19.5 T) dHvA measurements were performed using the field-modulation technique at the National Institute for Materials Science in Tsukuba; these experiments allowed for measurement as a function of field angle relative to the high symmetry directions and were performed using a dilution refrigerator with a lower temperature limit of 0.05 K. The intermediate field measurements were performed at a fixed angle using a He-3 refrigerator. The high-field ($B \leq 57$ T) dHvA signal was measured using the pulsed-field technique with counterwound highly compensated pickup coils in the 60 T short-pulse magnet at the National High Magnetic Field Laboratory in Los Alamos. The field angle was fixed for each sample, and the temperature was regulated between 0.5–1.5 K using a He-3 refrigerator.

The susceptibility and specific heat of $\text{Yb}_{1-x}\text{Lu}_x\text{Al}_3$ are shown in Fig. 1. The anomalies that are apparent below 40 K for YbAl_3 are suppressed and normal IV behavior is observed for $x \geq 0.05$. This result indicates

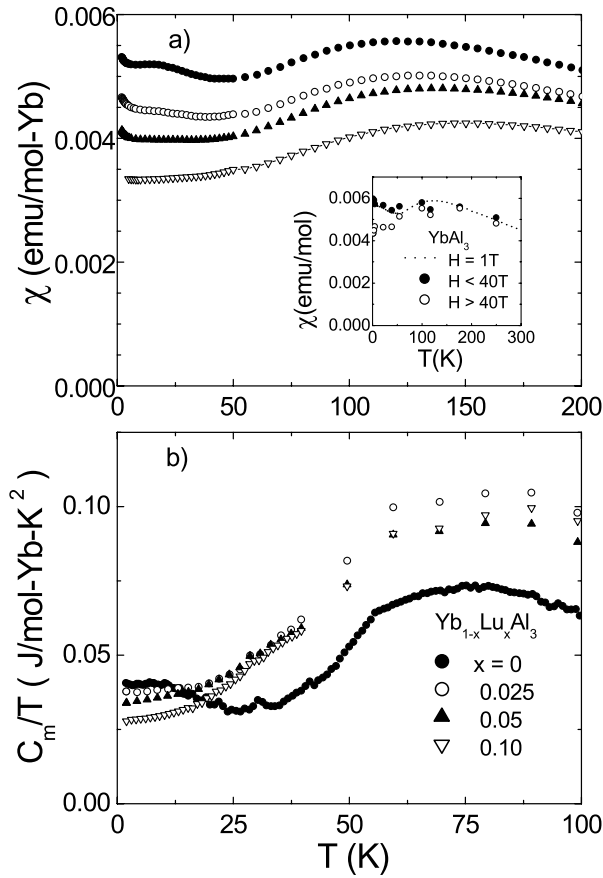


FIG. 1. (a) The susceptibility and (b) the specific heat coefficient for $\text{Yb}_{1-x}\text{Lu}_x\text{Al}_3$. (Symbols for different x are the same in both panels.) The inset compares the susceptibility of YbAl_3 in low and high magnetic fields (Ref. [2]).

a high sensitivity to alloy disorder and gives evidence that the anomalies require lattice coherence.

The dHvA frequencies for the low-field measurements are shown in Fig. 2. These reproduce the older work [4] with one nearly spherical high mass (23–29 m_e) branch, denoted β , and several branches that are confined to the vicinity of particular field directions. The frequencies for the intermediate field are essentially unchanged from those at low field. In Fig. 3(a) we show the fast Fourier transform (FFT) of the dHvA signal at high field ($45 < B < 55$ T) at 0.84 K and for a field along the $\langle 111 \rangle$ direction. Four peaks are resolved, which correspond in frequency to the α , β , ϵ , and η branches observed at low field [4]. The high-field frequencies are equal, within a few percent, to those observed at low field (Fig. 2) with the exception of the frequency of the β branch, which is 25% larger than at low field.

We analyzed the high-field measurements for each field range and temperature by fitting each FFT peak to the sum of a Gaussian and a second-order polynomial background function. We fit the Gaussian amplitudes to the function

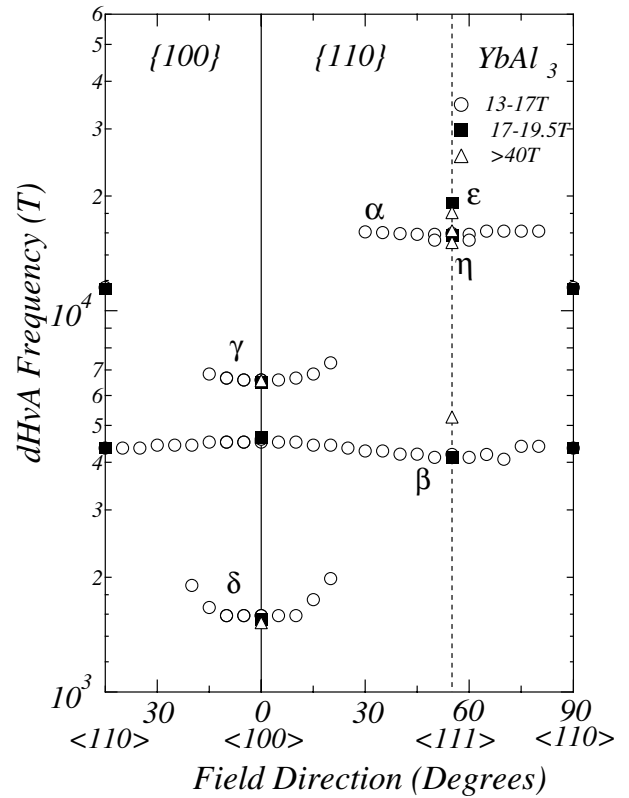


FIG. 2. The de Haas–van Alphen frequencies of YbAl_3 as a function of angle with respect to the high symmetry directions. The different symbols correspond to different field ranges for the measurement.

$$A(B, T) \propto \left(\frac{F^2 T}{B^{5/2}} \right) \left(\frac{\partial B}{\partial t} \right) \frac{\exp[14.7 m^* T_D / B]}{\sinh[14.7 m^* T / B]}, \quad (1)$$

where F is the dHvA frequency, m^* is the effective mass, and T_D is the Dingle temperature. This formula is appropriate for pulsed-field data [5]; a related expression appropriate for dc fields was used for the low and intermediate field data. By fitting at fixed field as a function of temperature we determined the effective mass for each branch and field range. Examples for the α and β branches are shown in Fig. 3(b). By fitting at fixed temperature as a function of field, we determine the Dingle temperature [Fig. 3(c)].

The masses determined from this analysis are plotted as a function of field in Fig. 4. The plot includes the low and intermediate field values, and data from two different samples for each field orientation at high field. The scatter at high field gives a good indication of both the reproducibility and the statistical error. Our key result is that the masses of the α and β branches for field along the $\langle 111 \rangle$ direction decrease by approximately a factor of 2 above 40 T. Somewhat smaller reductions are observed for the η and ϵ branches. For field along the $\langle 100 \rangle$ direction there is a more modest decrease of the γ mass and the mass of the δ branch appears to *increase* with field.

We did not observe a dHvA signal at high fields for the β branch for a field along either the $\langle 100 \rangle$ or the $\langle 110 \rangle$ direction. The low-field masses for this branch for these directions are 28.9 and $26.3m_e$, respectively. From Eq. (1) it is clear that large masses suppress the dHvA amplitude except at the lowest temperatures. In the pulsed-field measurement, the possibility of eddy current heating prohibits the study of metallic samples in a dilution refrigerator, restricting the accessible temperature range to $T > 0.5$ K. In this situation, it is very difficult to detect dHvA signals for branches with m^* much greater than

$15m_e$. Our data for a field in these directions are thus consistent with a lower limit on the high-field mass of order $15m_e$.

The field B^* for the transition to reduced masses is constrained by the dHvA data (Fig. 4) to lie somewhere in the interval $20 < B^* < 45$ T. The susceptibility (Fig. 4, inset) is constant up to 40 T, and decreases at higher field, suggesting that $B^* \sim 40$ T. The field dependence of the amplitude of the α branch fits the predicted Dingle curve for $B > 38$ T [Fig. 3(c)] which also suggests a transition field of this magnitude.

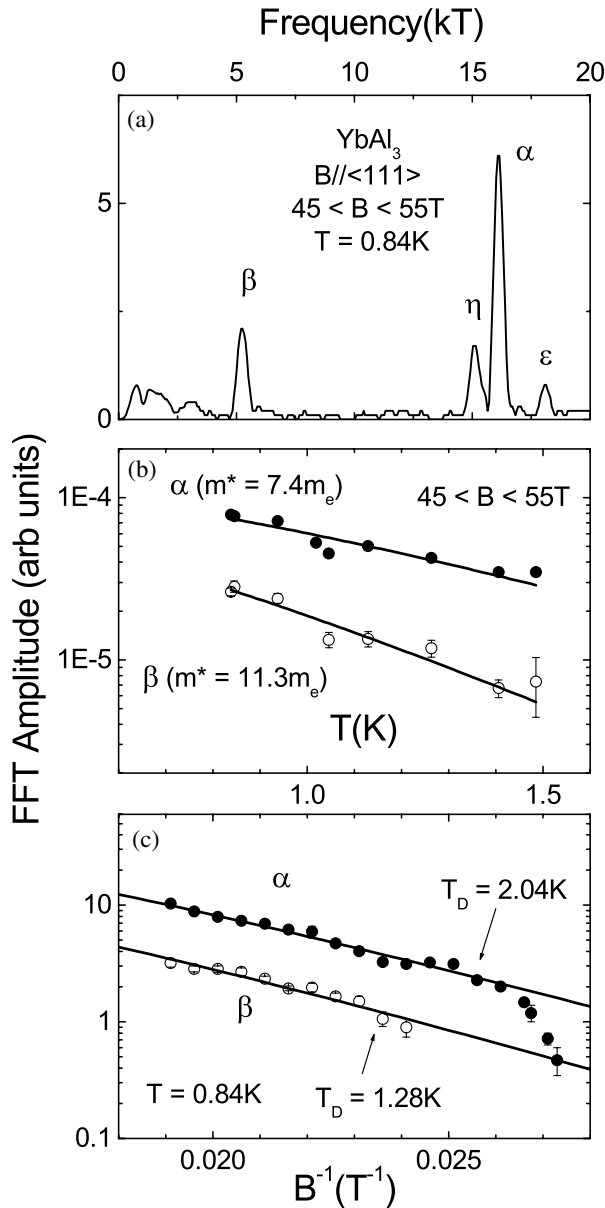


FIG. 3. (a) The fast Fourier transform of the de Haas–van Alphen spectrum at 0.84 K for a field along the $\langle 111 \rangle$ direction for fields in the range $45 \leq B \leq 55$ T. (b) A mass plot and (c) a Dingle plot for the α and β branches for a field along $\langle 111 \rangle$. (See text for the fitting function.)

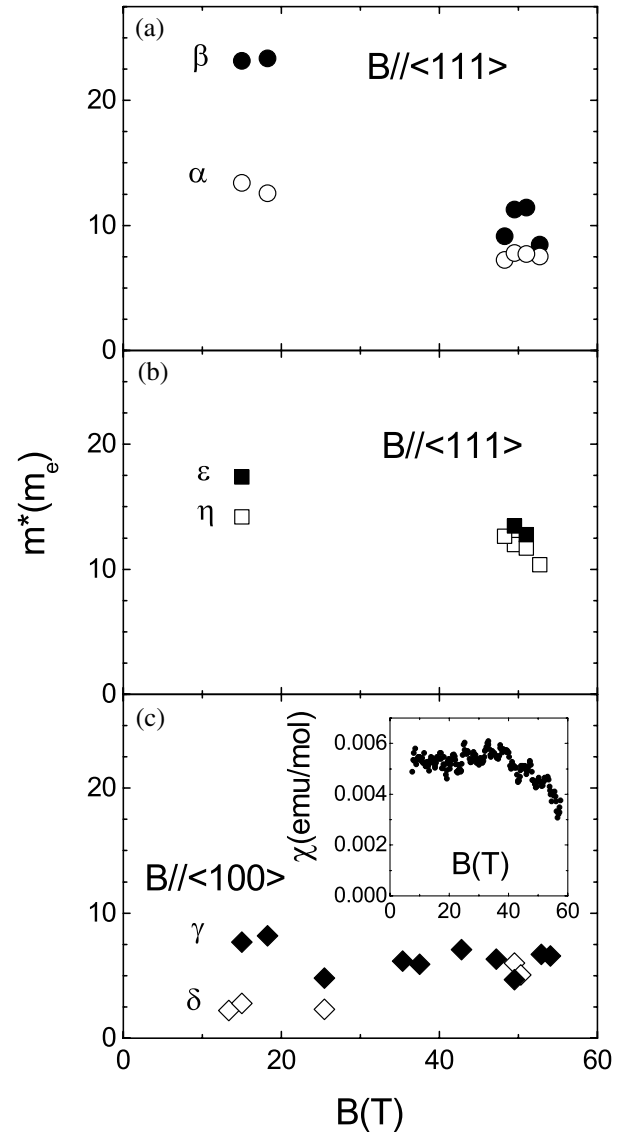


FIG. 4. The dHvA masses in units of the free electron mass m_e for different branches of the Fermi surface of YbAl_3 as a function of magnetic field for (a) and (b) fields along the $\langle 111 \rangle$ direction and (c) field along the $\langle 100 \rangle$ direction. A large reduction of the α and β branches is observed at high field. Inset: The field dependence of the magnetic susceptibility, showing that $\chi(B)$ decreases for $B > 40$ T.

The results reported here show that above a transition field $B^* \sim 40$ T the dHvA masses for key branches of Fermi surface decrease by approximately a factor of 2 for magnetic field parallel to $\langle 111 \rangle$, while masses for other branches and directions appear to be less affected by the field. From the effect of magnetic field on the susceptibility and the effect of alloy disorder on the specific heat (Fig. 1), we expect a 25% reduction of effective mass averaged over the Fermi surface. Our dHvA results are consistent with a decrease of this magnitude.

For heavy Fermion compounds with small Kondo temperatures, the application of a magnetic field larger than the Kondo field B_K (where $gJ\mu_B B_K = k_B T_K$) is known to cause a large reduction in the measured effective masses [5]. This finds a natural explanation in the theory of a Kondo impurity [6] or of the Anderson lattice [7]: when the Zeeman splitting becomes larger than the Kondo temperature, the $4f$ level polarizes; the resulting reduction of the spin degeneracy inhibits the Kondo interaction that is responsible for the large effective masses. For YbAl_3 where $g = 8/7$, $J = 7/2$, and $T_K = 670$ K, we then expect $B_K = 250$ T, much larger than the observed value of B^* . The theory [6] also predicts that the susceptibility will increase as the field increases in the vicinity of B_K ; and for heavy Fermions the $4f$ polarization gives rise to a continuous metamagnetic transition [8]. However, the susceptibility of YbAl_3 decreases at B^* . Finally, for systems such as CeRu_2Si_2 where the metamagnetic transition is observed experimentally, the Fermi surface alters at the transition because the polarization corresponds to a localization of the $4f$ electron which causes it to drop out of the Fermi volume [8]. For YbAl_3 , however, the transition has only a small effect on the Fermi surface geometry, with most frequencies unchanged but with a 25% increase in the frequency of the β branch along $\langle 111 \rangle$ which is suggestive of an increase in the Fermi volume. These facts suggest that the reduction of the masses is not connected with a simple polarization of the $4f$ level.

The transition field energy is, however, of the order of $k_B T_{\text{coh}}$, which suggests that the field dependence of the masses is connected to renormalization of the quasiparticle states and is intimately related to the suppression of the low temperature anomalies. For $B > B^*$ the susceptibility anomaly is suppressed and the temperature dependence becomes qualitatively similar to that of an Anderson impurity (Fig. 1, inset). The effective masses reduce to values that are still moderately large without much change in the Fermi surface geometry. It is as though the transition turns the compound into a non-anomalous intermediate valence compound, with moderately renormalized bands, but without $4f$ polarization.

In a $1/N_J$ -expansion treatment [9] of the Anderson lattice ($N_J = 2J + 1$), the coherence temperature was found to satisfy $T_{\text{coh}} \approx T_K/10$, which is approximately true for YbAl_3 . A low temperature anomaly in the sus-

ceptibility was predicted for $T < T_{\text{coh}}$ in the limit that the total electron density is close to the value appropriate for a Kondo insulator. A recent slave Boson treatment [10] of the Anderson lattice in the same limit shows that the ratio of $T^* = C_J/\chi(0)$ (where C_J is the Curie constant), T_{coh} , and T_K depends on the curvature of the bare density of states (DOS) at the Fermi level ϵ_F . When the DOS is flat at ϵ_F then $T^* = T_K$ and AIM behavior is observed. When the curvature is negative, then $T^* < T_K$ and $\chi(0)$ is enhanced over the AIM value. It remains to be seen whether such theory can explain the field dependence of the effective mass on the scale $k_B T_{\text{coh}}/\mu_B$ reported here.

The work by T.E. was supported by the Japanese Ministry of Education, the Inoue Science Promotion Foundation, and by Corning Japan. Work at UNLV was supported by the DOE EPSCoR-State/National Laboratory Partnership Award No. DE-FG02-00ER45835 and DOE Cooperative Agreement No. DE-FC08-98NV1341. The work by J.M.L. was supported by the Japanese Society for the Promotion of Science, by UCDRD funds provided by the University of California for the conduct of discretionary research by the Los Alamos National Laboratory, and by the UC/LANL Personnel Assignment Program. Work at the National High Magnetic Field Laboratory, Los Alamos Facility, was performed under the auspices of the National Science Foundation, the State of Florida, and the Department of Energy (DOE). Work at Los Alamos was supported by the DOE.

*Electronic address: jmlawren@uci.edu

- [1] J.M. Lawrence, P.S. Riseborough, C.H. Booth, J.L. Sarrao, J.D. Thompson, and R. Osborn, *Phys. Rev. B* **63**, 054427 (2001).
- [2] A.L. Cornelius, J.M. Lawrence, T. Ebihara, P.S. Riseborough, C.H. Booth, M.F. Hundley, P.G. Pagliuso, J.L. Sarrao, J.D. Thompson, M.H. Jung, A.H. Lacerda, and G.H. Kwei, *Phys. Rev. Lett.* **88**, 117201 (2002).
- [3] H. Okamura, T. Ebihara, and T. Nanba, *Acta Phys. Pol. B* **34**, 1075 (2003).
- [4] T. Ebihara, Y. Inada, M. Murakawa, S. Uji, C. Terakura, T. Terashima, E. Yamamoto, Y. Haga, Y. Onuki, and H. Harima, *J. Phys. Soc. Jpn.* **69**, 895 (2000).
- [5] N. Harrison, P. Meeson, P.-A. Probst, and M. Springford, *J. Phys. Condens. Matter* **5**, 7435 (1993).
- [6] P. Schlottmann, *Z. Phys. B: Condens. Matter* **51**, 223 (1983).
- [7] A. Wasserman, M. Springford, and A.C. Hewson, *J. Phys. Condens. Matter* **1**, 2669 (1989).
- [8] Y. Ōnuki, R. Settai, and H. Aoki, *Physica (Amsterdam)* **223B–224B**, 141 (1996).
- [9] Y. Ōno, T. Matsuura, and Y. Kuroda, *J. Phys. Soc. Jpn.* **60**, 3475 (1991).
- [10] S. Burdin and V. Zlatic, cond-mat/0212222.